

Hyperfine Quenching: Review of Experiment and Theory

W.R. Johnson

Abstract: We give a brief outline of the theory of hyperfine quenching followed by a review of the progress that has been made in both theory and experiment since the pioneering work of Garstang [J. Opt. Soc. Am. **52**, 845 (1962)].

PACS Nos.: 21.10.Ky, 32.10.Fn, 42.62.Fi

Key words: nuclear moments, hyperfine structure, beam-foil spectroscopy, laser spectroscopy.

1. Introduction

The role of the hyperfine interaction in reducing lifetimes of metastable states and, consequently, increasing the intensity of lines originating from such states was first noted in a comment by I. H. Bowen that was appended to a 1930 paper by Huff and Houston [1] who were studying the “forbidden” line at 2270 Å in the spectrum of mercury. The relevant part of the comment is:

Dr. Bowen has called our attention to the fact that the line $\lambda 2270$ in Hg is probably due to the coupling of the nuclear spin with the electronic angular momentum. An estimate based on the relative separation of the multiplets and the hyperfine structure gives the right order of magnitude for the intensity.

Although the correctness of Bowen’s conjecture was verified in experimental studies of Hg by Mrozowski [2], no progress in calculating intensities of hyperfine induced transitions was made until the seminal 1962 paper by Garstang [3] appeared. In that paper, rates of hyperfine induced transitions $^3P_0 \rightarrow ^1S_0$ and $^3P_2 \rightarrow ^1S_0$ were calculated for Mg, Zn, Cd, and Hg and it was shown that the calculated rates were in harmony with observations. It might be noted that Garstang’s calculations of hyperfine quenching rates in ^{25}Mg have been redone by several groups in recent years [4, 5] and the recent calculations agree with one another and with Ref. [3] at the 20% level.

Pioneering beam-foil measurements by Gould et al. [6] on hyperfine quenching in He-like V led to many measurements [7–19] and theoretical calculations [20–24] of quenching rates along the He isoelectronic sequence. Experimental lifetimes of $(1s2p) ^3P_0$ states along the He isoelectronic sequence differ from theoretical lifetimes by less than 10% typically. There have also been theoretical studies of hyperfine quenching for the Be, Mg, O, Ne, Ti, Ni and Zn isoelectronic sequences [5, 25–33]. However, for these sequences, there have been only four experimental measurements of quenching rates: Be-like N Brage et al. [34], Be-like Ti Schippers et al. [35, 36], Mg-like Al Rosenband et al. [37] and Ni-like Xe Träbert et al. [38].

Differences between theory and experiment for these ions are again 10%-20%. We will give a more detailed discussion of the aforementioned work later, but first we review the basic theoretical framework needed to evaluate hyperfine quenching rates. We set up the theory within the commonly used relativistic framework discussed by Schwartz [39].

2. Perturbation Theory & Radiation Damping

The Hamiltonian describing the interaction of an atomic electron with the electric and magnetic fields produced by a nucleus is

$$[1] \quad H_{\text{hfs}} = -\frac{e}{c} \boldsymbol{\alpha} \cdot \mathbf{A}(\mathbf{r}) + e\phi(\mathbf{r}),$$

where the dominant contributions to the electromagnetic potentials are from the nuclear magnetic dipole and electric quadrupole fields

$$[2] \quad \mathbf{A}(\mathbf{r}) = \frac{\boldsymbol{\mu} \times \mathbf{r}}{r^3} \quad \& \quad \phi(\mathbf{r}) = \sum_{ij} \frac{r_i r_j}{6r^5} Q_{ij}.$$

In the above, $\boldsymbol{\mu}$ is the nuclear magnetic moment operator and Q_{ij} are the Cartesian components of the nuclear quadrupole moment operator. Generally the nucleus has moments ranging from $k = 1$ to $2I$, where k is odd for magnetic moments and even for electric moments. Each of the terms in an expansion of the Hamiltonian in terms of moments can be written as a product of an irreducible tensor in the electron sector and an irreducible tensor in the nuclear sector. Thus

$$[3] \quad H_{\text{hfs}} = \left[-e \sum_{\lambda=1}^3 (-1)^\lambda \frac{i\sqrt{2} [\boldsymbol{\alpha} \cdot \vec{C}_{1\lambda}^{(0)}(\hat{r})]}{cr^2} \mu_{-\lambda} + e \sum_{\lambda=1}^5 (-1)^\lambda \frac{C_\lambda^2(\hat{r})}{r^3} Q_{-\lambda} + \dots \right] \\ = \sum_k T_k^{(e)} \cdot T_k^{(n)},$$

where the dots on the second line above represent magnetic octupole, electric hexadecapole and other higher-order terms. In the above, μ_λ and Q_λ are components of the moment operators in a spherical basis. The quantities $\vec{C}_\lambda^{(0)}(\hat{r})$ and $C_\lambda^2(\hat{r})$ are normalized vector and scalar spherical harmonics. There are

W.R. Johnson,¹ Department of Physics, 225 Nieuwland Science Hall, University of Notre Dame, Notre Dame IN 46556

¹Corresponding author (e-mail: johnson@nd.edu).

several important points to keep in mind in connection with the hyperfine interaction. Firstly, the total angular momentum $F = I + J$ is conserved. Secondly, an atomic level with angular momentum J splits into $\min(2I + 1, 2J + 1)$ sublevels with $F = I + J, F = I + J - 1, \dots, F = |I - J|$.

Let us designate an electronic state of angular momentum J by $|\gamma J M_J\rangle$. Here γ represents other quantum numbers such as multiplicity $(2S + 1)$ that distinguish between states with a given J . If we let H_0 represent the atomic Hamiltonian in the absence of the nuclear fields then

$$[4] \quad H_0|\gamma J M_J\rangle = E_{\gamma J}|\gamma J M_J\rangle.$$

In a similar way, we let H_{nuc} represent the nuclear Hamiltonian in the absence of electrons and let $|I, M_I\rangle$ represent a nuclear eigenstate. The Hamiltonian of the combined atom+nucleus system may then be written

$$[5] \quad H = H_0 + H_{\text{hfs}},$$

where we omit H_{nuc} since we ignore nuclear excitations entirely. Eigenstates of H are constructed from products of atomic and nuclear states coupled to form states with a specific value of F :

$$[6] \quad |(I, \gamma J) F M_F\rangle = \sum_{M_I, M_J} C(IM_I, JM_J, FM_F)|IM_I\rangle|\gamma J M_J\rangle.$$

An eigenstate of H is formed as a linear combination of coupled states (6) with the restriction that the nucleus remains in its ground state and the atomic states are limited to those in a specific fine-structure multiplet. The resulting expansion coefficients satisfy the eigenvalue equation

$$[7] \quad W_{\gamma J}^F C_{\gamma J, \gamma J}^F = \sum_{\gamma' J'} W_{\gamma' J, \gamma' J'}^F C_{\gamma' J', \gamma' J}^F,$$

where

$$[8] \quad W_{\gamma J, \gamma' J'}^F = E_{\gamma J} \delta_{\gamma, \gamma'} \delta_{J, J'} + \langle (I \gamma J) F | H_{\text{hfs}} | (I \gamma' J') F \rangle.$$

After standard angular momentum analysis, one finds

$$[9] \quad \langle (I \gamma J) F | H_{\text{hfs}} | (I \gamma' J') F \rangle = (-1)^{I+J+F} \sum_{k, \gamma' J'} \left\{ \begin{matrix} I & J & F \\ J' & I & k \end{matrix} \right\} \langle \gamma J || T_k^{(e)} || \gamma' J' \rangle \langle I || T_k^{(n)} || I \rangle,$$

where $\langle \gamma J || T_k^{(e)} || \gamma' J' \rangle$ and $\langle I || T_k^{(n)} || I \rangle$ are reduced matrix elements in the electronic and nuclear sectors, respectively. The nuclear matrix elements are

$$[10] \quad \langle I || T_1^{(n)} || I \rangle = \mu \sqrt{\frac{(I+1)(2I+1)}{I}},$$

$$[11] \quad \langle I || T_2^{(n)} || I \rangle = \frac{Q}{2} \sqrt{\frac{(I+1)(2I+1)(2I+3)}{I(2I-1)}}.$$

The electronic reduced matrix elements require detailed atomic structure calculations. Once such calculations have been made, one is in a position to solve Eq.(7) and obtain the expansion coefficients $C_{\gamma' J', \gamma J}^F$.

2.1. Perturbation Expansion

To the extent that second and higher order hyperfine effects are ignored, one can obtain the following simple expression for the expansion coefficients :

$$[12] \quad C_{\gamma' J', \gamma J}^F = (-1)^{I+J+F} \sum_k \left\{ \begin{matrix} I & J & F \\ J' & I & k \end{matrix} \right\} \times \frac{\langle \gamma J || T_k^{(e)} || \gamma' J' \rangle \langle I || T_k^{(n)} || I \rangle}{E_{\gamma J} - E_{\gamma' J'}}.$$

The diagonal expansion coefficient is $C_{\gamma J, \gamma J}^F = 1$.

2.2. Transition Matrix Elements and Line Strengths

With the mixing of states induced by the hyperfine interaction in mind, the line strength of the multipole transition from the atomic state $|\gamma J\rangle$ to the ground state $|^1S_0\rangle$ is given by

$$[13] \quad S_k^{(\lambda)}(F) = \delta_{Jk} \frac{[F]}{[k]} \left| \langle \gamma J || Q_k^{(\lambda)} || ^1S_0 \rangle + \sum_{\gamma' J' \neq \gamma J} C_{\gamma' J, \gamma' J'}^F \langle \gamma' J' || Q_k^{(\lambda)} || ^1S_0 \rangle \right|^2.$$

In the above, $Q_{kq}^{(\lambda)}$ is the multipole transition operator; k is the order of the multipole. The parameter λ is 1 for electric multipole transitions and 0 for magnetic multipole transitions. We use the notation $[k] = 2k + 1$.

Consider, for example, electric dipole transitions ($k=1$ and $\lambda = 1$) between $^3P_{0,2}$ states and the ground state. Note that there are four states in the multiplet containing the $J = 0, 2$ states: $^3P_{0,1,2}$ and 1P_1 . The first term on the right hand side of Eq.(13) vanishes since $J \neq k$. However, the two terms in the sum on the second line of Eq.(13), those associated with the 3P_1 and 1P_1 states, contribute to the sum and lead to a nonvanishing line strength for electric dipole transitions between the excited $J = 0, 2$ states and the 1S_0 ground state. (This is in apparent violation of Laporte's rule [40]). It should be noted that the line strength in Eq.(13) depends not only on the initial state γJ but also on the particular hyperfine sublevel F of the state γJ . For the special case $J = 0$, there is a single hyperfine level $F = I$ and, therefore, a unique line strength.

The transition rate (in atomic units) is given by

$$[14] \quad A_k^{(\lambda)}(F) = \frac{(2k+2)(2k+1)}{k[(2k+1)!!]^2} \left(\frac{\omega}{c}\right)^{2k+1} \frac{S_k^{(\lambda)}(F)}{[F]},$$

where $\omega = E_{\gamma J} - E_{^1S_0}$ is the transition energy.

2.3. Example: Decay of the $(1s2p)^3P_0$ state of He-like P

Phosphorus has only one stable isotope ^{31}P , which has nuclear spin $I = 1/2$ and nuclear magnetic moment $\mu = 1.1316$. The 3P_0 state of He-like P nominally decays to the lower 3S_1 state by E1 emission. However, owing to mixing of states within the $(1s2p)$ multiplet, the 3P_0 state acquires a small admixture of 1P_1 and 3P_1 states which decay to the 1S_0 ground state by

Table 1. Contributions to decay rates (ns^{-1}) of $(1s2p)^3P_{2,0}$ states in He-like P. Theory from Ref. [23]

Mode	3P_2	3P_0
$E1 \rightarrow 2^3S_1$	0.2214	0.1659
$M2 \rightarrow 1^1S_0$	0.0689	0.0000
Induced $E1 \rightarrow 1^1S_0$	0.0037	0.0409
A_{tot}	0.2940	0.2068
Expt. Ref. [10]	0.298(4)	0.205(4)

E1 emission. The expansion coefficients for the 3P_0 state given in Eq. (12) are

$$C_{30,31}^{1/2} = -0.0096974$$

$$C_{30,11}^{1/2} = 0.00014187,$$

and the corresponding reduced dipole matrix elements (a.u.) are

$$\langle ^3P_1 \| Q_1^1 \| ^1S_0 \rangle = 0.00944595$$

$$\langle ^1P_1 \| Q_1^1 \| ^1S_0 \rangle = -0.119197315,$$

leading to the following results for the induced E1 line strength and transition rate, respectively:

$$S_1^{(1)} = 1.17748 \times 10^{-8} \text{ (a.u.)}$$

$$A_1^{(1)} = 4.09 \times 10^7 \text{ (1/s)}.$$

Total rates for decay of 3P_0 and 3P_2 states in He-like P, including contributions of hyperfine quenching and other decay channels, are given in Table 1. For the 3P_0 state, hyperfine quenching contributes 25% of the total rate, while for the 3P_2 state, quenching contributes only 1.2% which is comparable to the experimental error. The quenching rate for the 3P_2 state has been averaged over hyperfine components assuming that the hyperfine states are statistically occupied. For both transitions, theory and experiment are seen to be in agreement.

2.4. Example: Decay of the 3P_0 state of He-like Ag

Silver has two stable isotopes with nonvanishing nuclear spin, ^{107}Ag and ^{109}Ag . For both isotopes, $I = 1/2$. Comparing the theory developed in the above paragraphs with experimental measurements [14, 15], we obtain the following lifetimes (ps) of 3P_0 states:

Ag^{107}	Theory: 2.607	Expt: 3.97(37),
Ag^{109}	Theory: 1.963	Expt: 2.84(32).

To understand these discrepancies, we first note that the 3P_0 and 3P_1 energy levels cross near $Z = 47$ resulting in the fact that the width Γ_{31} of the $^3P_1 - ^1S_0$ transition is comparable to the energy separation $E_{10} = E(^3P_1) - E(^3P_0)$. This fact is illustrated in Fig. 1.

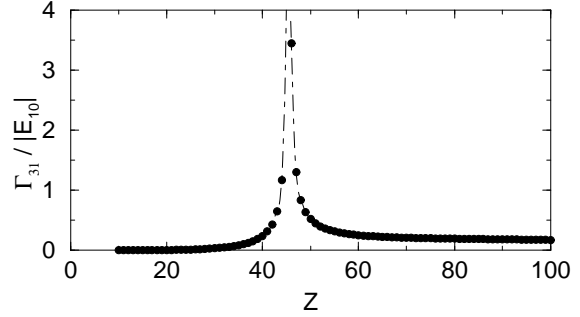


Fig. 1. Ratio of the linewidth of the 3P_1 transition to the $^3P_0 - ^3P_1$ energy separation $|E_{10}|$ along the He isoelectronic sequence.

2.5. Radiation Damping Potential

The implication of the fact that the transition line width is larger than or comparable to the fine-structure separation is that the radiation field can no longer be treated as a small perturbation but must be included along with the hyperfine interaction in the interaction Hamiltonian. To address this problem, a complex energy matrix was introduced by Indelicato et al. [21] in which both hyperfine and radiative effects are taken into account at the same level of approximation. The radiation damping method provides a generalization of the complex energy matrix that reduces to the previously discussed perturbation theory away from level crossings. Below, we outline the radiation damping method following closely the discussion given in Ref. [23].

One particularly convenient method for including radiative corrections in atomic wave functions is by means of the nonlocal optical potential V_{rd} introduced by Robicheaux et al. [41]. If we let $Q_{kq}^{(\lambda)}$ represent the electromagnetic multipole transition operator, then

$$[15] \quad V_{\text{rd}}|\psi_E\rangle = ie^2 \sum_{kq\lambda} \frac{(k+1)(2k+1)}{k[(2k+1)!!]^2} \sum_n (E - E_n) k_n^{2k} Q_{kq}^{(\lambda)} |\psi_n\rangle \langle \psi_n | Q_{kq}^{(\lambda)\dagger} |\psi_E\rangle,$$

where $k_n = (E - E_n)/c$. The potential V_{rd} is an antihermetian matrix. Among the states $^3P_{0,1,2}$, 1P_1 there are four diagonal matrix elements and one distinct off-diagonal matrix element of V_{rd} . The diagonal matrix elements may be written

$$[16] \quad \langle 2^{\gamma}P_J | V_{\text{rd}} | 2^{\gamma}P_J \rangle = \frac{i}{2} \sum_{k\lambda} \sum_n \hbar A_k^{(\lambda)} (2^{\gamma}P_J \rightarrow n),$$

where the sum is over all lower states n . The off-diagonal matrix element is

$$[17] \quad \langle 2^3P_1 | V_{\text{rd}} | 2^1P_1 \rangle = i \frac{\hbar}{2} \left[\frac{4}{9} k_0^3 \langle 1^1S_0 \| Q_1 \| 2^1P_1 \rangle \langle 1^1S_0 \| Q_1 \| 2^3P_1 \rangle + \frac{4}{9} k_1^3 \langle 2^3S_1 \| Q_1 \| 2^1P_1 \rangle \langle 2^3S_1 \| Q_1 \| 2^3P_1 \rangle \right].$$

Including V_{rd} together with $H_0 + H_{hf}$ in Eq.(7) leads to a complex generalization of the 4×4 hyperfine energy eigenvalue equation. The real parts of the eigenvalues give the energies of the hyperfine levels while the imaginary parts give half-widths of transitions from the 3P_J states to lower states. (It should be noted that the energy E used to evaluate $k_n = (E - E_n)/c$ in Eqs. (16,17) is the energy of the state 3P_0 or 3P_2 being quenched.) For cases where the radiative half-widths of the levels are small compared to the fine-structure intervals, the eigenvalues of the complex matrix reduce to the results of perturbation theory given in the previous section. It should be emphasized that the coherent combinations of the two $J=1$ amplitudes that occur in the limiting case are a consequence of the fact that *off-diagonal* contributions are included in the complex energy matrix.

If we limit our calculation to a 2×2 complex matrix coupling only the 3P_0 and 3P_1 states, the radiation damping approach reduces to the complex matrix approach used by Indelicato et al. in Ref. [21] to evaluate quenching rates for the $J = 0$ states in He-like ions. This formulation gives approximately correct quenching rates for He-like ions in the range $Z \approx 40$ where interference between the singlet and triplet $J = 1$ amplitudes contributes only a few percent to the decay rate. As shown in the following comparison, theory is brought into agreement with experiment for the case of ${}^{107}\text{Ag}$ and ${}^{109}\text{Ag}$ discussed earlier when the perturbative treatment of the radiation field is replaced by the radiation damping method.

$$\begin{array}{ll} \text{Ag}^{107} & \text{Rad. Damp.: } 3.724 \quad \text{Expt: } 3.97(37), \\ \text{Ag}^{109} & \text{Rad. Damp.: } 2.810 \quad \text{Expt: } 2.84(32). \end{array}$$

Our recommendation is to treat hyperfine quenching using the perturbative approach described in Subsections 2.1 & 2.2 except near level crossings, where the radiation damping approach is more appropriate.

3. He-like ions

As mentioned in the Introduction, following the experiment of Gould et al. [6] in which hyperfine quenching effects were observed in the decay of the 3P_2 state in the He-like ion ${}^{51}\text{V}$, many theoretical and experimental papers concerning hyperfine quenching in metastable states of He-like ions appeared. Below, we list and comment on the theoretical papers on hyperfine quenching in helium-like ions. We use the headings PT or RD to designate calculations carried out using perturbation theory or radiation damping, respectively.

He-like Ions Theory:

PT Mohr [20] calculates quenching rates for 3P_0 states of helium like ions using a $1/Z$ expansion including Breit-Pauli corrections for relativistic effects as well as corrections for the Lamb shift. A table of induced transition rates for ions with $9 \leq Z \leq 29$ is given.

RD Indelicato et al. [21] calculate quenching rates for 3P_0 states of He-like ions using a 2×2 version of the radiation damping method. Matrix elements and energies are evaluated using the multi-configuration Dirac Fock (MCDF) method including the Breit interaction and the

Table 2. Comparison of theory & experiment for lifetimes of ($1s2p$) 3P_0 states in He-like ions. Lifetimes are in ns for the first four ions and in ps for the remaining five ions. Theoretical lifetimes are from Ref. [23]

Ion	I	μ_I	Expt.	Theory	Ref.
${}^{19}\text{F}$	1/2	2.6289	9.48(20)	9.574	[7, 8]
${}^{27}\text{Al}$	5/2	3.6415	4.80(20)	4.695	[9]
${}^{31}\text{P}$	1/2	1.1316	4.88(9)	4.836	[10, 11]
${}^{61}\text{Ni}$	3/2	-0.75002	0.470(5)	0.4455	[12, 13]
${}^{107}\text{Ag}$	1/2	-0.11368	3.98(37)	3.724	[14, 15]
${}^{109}\text{Ag}$	1/2	-0.13069	2.84(32)	2.810	[14, 15]
${}^{155}\text{Gd}$	3/2	-0.25810	13.43(27)	13.57	[17]
${}^{157}\text{Gd}$	3/2	-0.33860	7.65(55)	8.01	[17]
${}^{197}\text{Au}$	3/2	0.14816	22.16(81)	23.31	[18, 19]

Lamb shift. Ions with $Z = 46 - 92$ are considered. By treating the fine-structure energy interval $E_{10} = E({}^3P_1) - E({}^3P_0)$ as an adjustable parameter in the 2×2 energy matrix, it is shown that an accurate measurement of the 3P_0 lifetime can lead to an accurate value for E_{10} . An experiment based on this idea was later carried out on isotopes of Ag by [14], leading to a value of E_{10} in good agreement with theoretical predictions.

PT Aboussaïd et al. [22] used perturbation theory to evaluate quenching rates for 3P_0 states of the He-like ions ${}^{19}\text{F}$, ${}^{23}\text{Na}$ and ${}^{25}\text{Al}$. The multi-configuration Hartree-Fock (MCHF) method with Breit-Pauli corrections was used to calculate energies, wave functions and matrix elements. The resulting transition rates were 10%-15% larger than those obtained in Ref. [20].

RD Johnson et al. [23] carried out PT and RD calculations of hyperfine quenching rates of 3P_0 and 3P_2 levels in He-like ions with $Z=6-100$. Energies and matrix elements were evaluated using the relativistic CI method including the Breit interaction and Lamb shift. The 3P_0 rates for low- Z elements are in close agreement with [20] while for high- Z elements, the results are in agreement at the 10% level (some exceptions) with the calculations of [21]. Averages over hyperfine sublevels (assuming statistical occupation) are given for the 3P_2 decay rates.

PT Volotka et al. [24] carry out perturbation theory calculations of quenching rates for 3P_0 and 3P_2 levels in He-like ions $Z = 15 - 30$. The results are presented using a $1/Z$ expansion. Effects of the Coulomb and Breit interactions are included to order $(\alpha Z)^2/Z$. The resulting rates are in excellent agreement with those given in Refs. [20] and [23].

He-like Ions Experiment:

- Engström et al. [7] & [8] made beam-foil measurements of the lifetimes of the 3P_0 and 3P_2 levels of the He-like ion ${}^{19}\text{F}$ at the 3 MV Pelletron tandem accelerator at the University of Lund. The result for the 3P_0 level, where the induced E1 rate contributes 15% to the total rate is compared with theory in Table 2. For the 3P_2 state, where

hyperfine quenching is negligible, the experimental lifetime $\tau = 10.44(0.15)$ ns is in excellent agreement with the theoretical result 10.33 ns.

- Denne et al. [9] carried out beam-foil measurements of lifetimes of the 3P_0 and 3P_2 levels of the He-like ion ^{25}Al at the 6.4 MV EN Tandem Accelerator in Upsala. The measured lifetime of the 3P_0 state, where quenching contributes 30% of the total, is seen in Table 2 to be in agreement with theory. Hyperfine quenching contributes only 3% to the total lifetime for the 3P_2 state and this experiment gives $\tau = 5.40(0.20)$ ns compared with the theoretical value 5.165 ns.
- Jasper et al. [10] and Livingston and Hinterlong [11] made beam-foil measurements of lifetimes of the 3P_0 and 3P_2 states in He-like ^{31}P at the Notre Dame Tandem Accelerator facility. For the 3P_0 state, where quenching contributes 25% to the total rate, the measurement agrees with theory. Quenching contributes only 1% to the decay rate of the 3P_2 state and again theory and experiment are in good agreement as seen in Table 1.
- Dunford et al. [12, 13] made beam-foil measurements on ^{58}Ni and ^{61}Ni at the Argonne van de Graaf-Linac (ATLAS) facility and found clear evidence for hyperfine quenching of the 3P_0 level in ^{61}Ni . For ^{61}Ni they obtained the lifetime $\tau = 470(50)$ ps given in Table 2. Using the version of the radiation-damping technique described in [21], the $^3P_0 - ^3P_1$ energy interval was found to be $E_{10} = 2.33(15)$ eV. This value is in agreement with the theoretical value $E_{10} = 2.323$ eV from Ref. [23].
- Marrus et al. [14] and Birkett et al. [15] performed beam-foil measurements of lifetimes of 3P_0 states in He-like ^{107}Ag and ^{109}Ag at the UNILAC accelerator at GSI giving values $\tau(107) = 3.98(37)$ ps and $\tau(109) = 2.94(32)$ ps shown in Table 2. The $^3P_0 - ^3P_1$ fine-structure interval was found to be $|E_{10}| = 0.79(04)$ eV using the 2×2 radiation damping technique [21]. This experimental value can be compared to the theoretical value 0.8014 eV from [23]. Additionally, Simionovici et al. [16] measured lifetimes of 3P_2 states in He-like Ag ions as $\tau = 1.24(0.11)$ ps compared with the theoretical value $\tau = 1.094$ ps [23]. Unfortunately, for both ions, hyperfine quenching contributes less than 0.05% to the lifetime of 3P_2 states.
- Indelicato et al. [17] obtained lifetimes of 3P_0 states in He-like ions ^{155}Gd and ^{157}Gd from beam-foil time of flight measurements made at the GANIL accelerator (Caen, France). The resulting experimental lifetimes $\tau(155) = 13.43(27)$ ps and $\tau(157) = 7.65(55)$ ps are compared with theory in Table 2. The measured lifetimes were combined following Ref. [21] to give $E_{10} = 18.57(19)$ eV for the $^3P_0 - ^3P_1$ fine-structure interval; the corresponding theoretical value is 18.57 eV [23].
- Toleikis et al. [18, 19] measured the lifetime of the 3P_0 state of the He-like ion ^{197}Au at the GSI accelerator facility using the beam-foil time of flight method giving the result $\tau = 22.16(81)$ ps shown in Table 2. It should be mentioned that the theoretical value shown in Table 2

Table 3. Theoretical 3P_2 rates (ns^{-1}) for He-like ions in cases where hyperfine quenching contributes $> 5\%$ and where the lifetime $\tau > 1$ ps.

	μ_I	I	A_{M2+E1}	A_{hf}	A_{tot}	% from hfs
^{45}Sc	4.7565	7/2	1.693	0.3928	2.085	23
^{50}V	3.3457	6	3.188	0.3622	3.550	11
^{51}V	5.1487	7/2	3.188	0.9453	4.133	29
^{51}Mn	3.5683	5/2	5.891	0.9584	6.850	16
^{55}Mn	3.4687	5/2	5.891	0.9056	6.797	15
^{59}Co	4.6270	7/2	10.59	2.733	13.33	25
^{63}Cu	2.2273	3/2	18.49	1.453	19.94	7
^{65}Cu	2.3816	3/2	18.49	1.662	20.15	8
^{69}Ga	2.0166	3/2	31.31	2.035	33.35	6
^{71}Ga	2.5623	3/2	31.31	3.285	34.60	10
^{79}Br	2.1064	3/2	82.74	5.908	88.65	7
^{81}Br	2.2706	3/2	82.74	6.865	89.61	8
^{87}Rb	2.7515	3/2	129.6	15.83	145.4	12
^{93}Nb	6.1705	9/2	298.5	134.9	433.4	45
^{99}Tc	5.6847	9/2	440.6	169.3	609.9	38

contains corrections for the Bohr-Weisskopf effect [42] and for two-photon (E1M1) emission [43] as discussed in [19].

Decay of 3P_2 states in He-like ions:

For most of the He-like ions discussed earlier, the hyperfine induced contribution has given a small or negligible contribution to lifetimes of 3P_2 states. As an aid to choosing He-like ions for which the hyperfine quenching gives a significant contribution to the total, we list in Table 3 those He-like ions for which the 3P_2 lifetime $\tau > 1$ ps and the fractional contribution of hyperfine quenching is $> 5\%$. It is interesting to note that for He-like ^{51}V , the ion studied in the work of Gould et al. [6], hyperfine quenching is responsible for 29% of the total decay rate.

4. Be-like ions and Mg-like ions

Beyond the He isoelectronic sequence, the most studied systems are Be-like and Mg-like ions. From an abstract point of view, Be and Mg isoelectronic sequences are both simpler than the He sequence since there is no counterpart of the 3S_1 state interposed between the lowest $nsnp$ multiplet and the $(ns)^2\ ^1S_0$ ground state. The 3P_0 state decays to the 1S_0 ground state through the hyperfine induced E1 channel with competition only from the highly retarded two-photon E1M1 channel. Similarly, the only competing channel for the hyperfine induced decay of the 3P_2 state is single-photon M2 decay to the ground state. The primary challenge for theory in the case of these more complex ions is to obtain accurate wave functions and transition energies. This challenge is simply met for highly charged ions since correlation corrections fall off as inverse powers of the nuclear charge Z . However, near the neutral end of each sequence, adequate treatment of correlation usually presents computational difficulties. Despite the simplicity of these ions, there have been only two measurements of hyperfine quenching for Be-like ions and only one measurement for Mg-like ions. Moreover, the precision of these measurements is not sufficiently

high to provide a stringent test of the available calculations.

4.1. Be-like Ions

RD Marques et al. [44] were the first to carry out calculations for Be-like ions. Energies and wave functions were evaluated using the MCDF method and included corrections for the Breit interaction and QED. Correlation corrections were included in the 1S_0 ground state but not in the $(2s2p)$ states. The 2×2 complex matrix method, introduced in [21], was used to determine the 3P_0 transition rate. Inasmuch as contributions from the 1P_1 state which add coherently with those from the 3P_1 state are ignored, one would expect rather large errors in these calculations, as confirmed in the comparisons shown in Table 4.

PT Brage et al. [27] carried out MCHF calculations with Breit-Pauli corrections and MCDF calculations of hyperfine quenching rates of 3P_0 transition rates in Be-like and Mg-like ions. The calculations are made for elements of astrophysical importance. For Be-like ions, these calculations agree to 10-15% with the more accurate calculations of Refs. [45, 46]. A proposal is made to obtain isotope abundances by using the 3P_0 transition rates in connection with spectroscopic data from planetary nebulae.

PT Cheng et al. [45] made relativistic CI calculations including Breit and QED corrections for 3P_0 quenching rates for Be-like ions, $Z=6$ to 92. The calculations were carried out using both perturbation theory and the radiation damping method and the two methods yielded identical results. The rates obtained agree with those obtained in [46]. However, the prediction for the 3P_0 decay rate in ^{47}Ti [0.673 s^{-1}] disagrees significantly with the experimental rate [$0.56(3) \text{ s}^{-1}$] obtained in [35, 36].

PT Andersson et al. [46] carried out MCDF calculations, including Breit and QED corrections of quenching rates for 3P_0 and 3P_2 states of Be-like ions having nuclear charges in the range $Z = 6$ to 22. Careful attention was given to the treatment of correlation effects. For 3P_0 states these calculations are in agreement with the calculations of Ref. [45].

Expt. Brage et al. [34] obtained an experimental value for the 3P_0 quenching rate in N from spectroscopic observations of the planetary nebula NGC3918 made using the STIS instrument on the Hubble Space Telescope. The observed rate is $4(1.3) \times 10^{-4} \text{ s}^{-1}$. Both isotopes ^{14}N and ^{15}N have nuclear spin $I \neq 0$. For ^{14}N , the theoretical transition rate is $4.40 \times 10^{-4} \text{ s}^{-1}$, while for ^{15}N it is $3.27 \times 10^{-4} \text{ s}^{-1}$. The error in the experimental rate is large enough to cover any possible abundance ratio for the two isotopes.

Expt. Schippers et al. [35, 36] employed resonant electron-ion recombination in the heavy-ion storage ring TSR at the Max-Planck Institute for Nuclear Physics, Heidelberg, Germany to monitor the time dependent population of the 3P_0 state in Be-like ^{47}Ti . The observed transition

Table 4. Theoretical and experimental transition rates (s^{-1}) are compared for $^3P_0 - ^1S_0$ transitions in Be-like ions.

Method	^{14}N	^{15}N	^{47}Ti	Ref.
RD		9.47[-5]	0.356	[44]
PT	4.92[-4]	3.62[-4]		[27]
PT & RD	4.44[-4]	3.27[-4]	0.673	[45]
PT	4.44[-4]	3.27[-4]	0.677	[46]
Expt.	4.0(1.3)[-4]	4.0(1.3)[-4]		[34]
Expt.			0.56(3)	[35, 36]

Table 5. Comparison of calculations of the 3P_0 transition rate (s^{-1}) in the Mg-like ion Al^+ with experiment.

Method	rate(s^{-1})	Ref.
RD	2.65[-2]	[25]
PT	4.33[-2]	[47]
PT	4.40[-2]	[5]
Expt.	4.85(20)[-4]	[37]

rate is $0.56(3)\text{s}^{-1}$ which differs significantly from the theoretical rate 0.673s^{-1} .

4.2. Mg-like Ions

RD Marques et al. [25] carried out MCDF calculations including Breit and QED corrections of transition rates for $(3s3p)^3P_0$ levels in Mg-like ions with nuclear charges $Z=14-92$ using a 2×2 complex matrix method.

PT As mentioned previously, Brage et al. [27] carried out MCHF calculations with Breit-Pauli corrections and MCDF calculations of hyperfine quenching rates of 3P_0 transition rates in Be-like and Mg-like ions. These calculations did not include Al^+ , the only Mg-like ion for which an experimental quenching rate is available.

PT Kang et al. [47] carried out MCDF calculations of quenching rates for the 3P_0 states of Mg-like ions ($Z=13-78$) including Breit and QED corrections.

PT Andersson et al. [5] carried out MCDF calculations including Breit and QED corrections of quenching rates for 3P_0 and 3P_2 states of Mg-like ions ($Z=12-31$). These calculations differ substantially from those of Ref. [47] primarily because of a more careful treatment of correlation.

Expt. Rosenband et al. [37] applied laser spectroscopy to study the $^1S_0 - ^3P_0$ clock transition in $^{27}\text{Al}^+$. A single aluminum ion was confined together with a single beryllium ion in a linear Paul trap. The clock transition frequency was measured to be $\nu = 1\,121\,015\,393\,207\,851(6)$ Hz and the lifetime of the 3P_0 state was measured to be $\tau = 20.6 \pm 1.4$ s.

Table 6. Hyperfine induced transition rates (s^{-1}) for 3P_0 states in alkaline earth atoms and for Yb. Rates listed here are from Ref. [4].

Atom	I	μ_I	Q (b)	$A[^3P_0]$ (s^{-1})
^{25}Mg	5/2	-0.85546	0.1994(20)	4.44[-4]
^{43}Ca	7/2	-1.31727	-0.0408(8)	2.22[-3]
^{87}Sr	9/2	-1.09283	0.335(20)	7.58[-3]
^{171}Yb	1/2	0.4919		4.35[-2]
^{173}Yb	5/2	-0.6776	2.800(40)	3.85[-2]

5. Neutral Atoms

The transitions $^3P_0 - ^1S_0$ and $^3P_2 - ^1S_0$ in neutral alkaline earth atoms are candidates for ultra-precise atomic clocks since the ratio of the line widths to the transition energies $A[^3P_0]/\Delta E \sim 10^{-18}$. Calculations of the transition rates for the 3P_0 and 3P_2 states were carried out by Porsev and Derevianko [4] for the atoms Mg, Ca, Sr, and Yb and their results for the 3P_0 rate are shown in Table 6. These calculations were done using a relativistic version the CI + MBPT method in which valence-valence correlations are included using the CI method while valence-core and core-core correlations are included by modifying the two-particle Hamiltonian H_0 by the Coulomb self-energy operator $\Sigma(E)$, leading to an effective Hamiltonian

$$[18] \quad H = H_0 + \Sigma(E).$$

For Be-like Mg, Garstang [3] obtained $A[^3P_0] = 4.2[-4]$ (s^{-1}) and Andersson et al. [5] obtained $5.00[-4]$ (s^{-1}). It is a bit unsettling that the various theoretical lifetimes differ by such a large amount. Differences between various determinations of $A[^3P_2, F]$ have a similar spread.

6. Ni-like Ions

In the absence of the hyperfine interaction, the lowest excited level ($3d^9 4s$) 3D_3 of a Ni-like ion can decay to the $3d^{10} 1S_0$ Ne-like ground state only by M3 emission. In Träbert et al. [48], the measured lifetime ($\tau = 11.5 \pm 0.5$ ms) for naturally occurring Ni-like Xe was found to be significantly shorter than the theoretical M3 rate (15.12 ms). The shortening was clearly due to hyperfine quenching, given that naturally occurring Xe is a mixture of isotopes nearly half of which have $I \neq 0$. To clarify the situation, Träbert et al. [49] made separate measurements of the 3D_3 lifetime for isotopically pure ^{129}Xe and ^{132}Xe . For the isotope ^{132}Xe ($I=0$), the measured lifetime 15.03 ± 0.24 ms agreed well with the theoretical M3 value. For Ni-like ^{129}Xe ($I=1/2$), the $F=5/2$ sublevel of the 3D_3 level is quenched by mixing with 1,3D_2 states while the $F=7/2$ sublevel decays by M3 emission only. By fitting the decay curve to a double exponential

$$[19] \quad N[^3D_3](t) = N_{7/2}(0)e^{-\Gamma_{M3} t} + N_{5/2}(0)e^{-(\Gamma_{M3} + \Gamma_{E2hf}) t},$$

lifetimes of individual F sublevels were determined. The lifetime of the $F = 7/2$ sublevel was found to be 15.1 ± 0.5 ms

in agreement with the theoretical M3 lifetime. The lifetime of the quenched $F = 5/2$ state was found to be 2.7 ± 0.1 ms, in agreement with the quenched rate 2.84 ms obtained by Yao et al. [50].

7. Other Cases

- Ti-like** (Theory only) Ions of the Ti isoelectronic sequence have a ground state configuration $(4d)^2 5D_J$. For high Z ions, the the $J=4$ level is below below the $J=3$ and 2 levels but above the $J = 1$ and 0 levels. In ions with $I = 0$, the $J=4$ level can decay to lower levels only by highly retarded M3 or E4 radiation, However, for ions with $I \geq 1$, the $J=4$ level mixes with the $J = 2$ through the $k = 2$ contribution to H_{hf} and decays to the ground state by E2 emission. It is proposed in Parente et al. [26] and Indelicato [33] to use the measured rate which is very sensitive to the nuclear electric-quadrupole moment, as a new method for measuring quadrupole moments.
- Zn-like** (Theory) Hyperfine quenching of $4p4s$ 3P_0 levels in Zn-like ions $Z=30-92$ were evaluated using MCDF wave functions and the radiation-damping method by Marques et al. [29].
- Zn-like** (Expt.) Dielectronic recombination of Zn-like Pt ions was measured at the Heidelberg heavy-ion storage ring TSR. Pronounced differences were observed in the resonance structure of ^{194}Pt and ^{195}Pt . These differences were attributed to the presence of $(4s4p)$ 3P_0 components in the Zn-like ^{194}Pt beam. The $(4s4p)$ 3P_0 component is quenched in the ^{194}Pt beam. Schippers et al. [51]
- O-like** (Theory) Calculations of energy levels and transition rates for states in the $2p^4$ configuration of O-like ions with $20 \leq Z \leq 30$ were made by Marques et al. [52]. It was shown that the hyperfine induced E1 contribution is negligible.
- Ne-like** (Theory) Calculations of quenching of the $(2p)^5 3s$ 3P_2 and $(2p)^5 3s$ 3P_0 levels of Ne-like ions were made for $Z=13-79$ were made by Andersson et al. [31].
- Radium** (Theory) MCDF calculations of the decay of the $7s7p$ 3P_0 state through 2-photon E1M1 and hyperfine induced channels were made Bieron et al. [53]
- XeII** (Expt.) Using a state selective laser probing technique for lifetime measurement in the ion storage ring CRYRING at the Manne Siegbahn Laboratory, evidence for a drastic differences between the decay rates of the hyperfine states of the metastable level $(5p)^4 5d^4 D_{7/2}$ in $^{129}\text{Xe}^+$ was found by Mannervik et al. [54].

8. Conclusions

- There are two methods “perturbation theory” and “radiation damping method” available for calculating hyperfine quenching rates. The rates obtained by the two methods agree far away from level crossing. The radiation damping theory is appropriate near level crossing.

- Decays from $(1s2p)^3P_0$ levels in He-like ions have been thoroughly studied theoretically and experimentally. Experimental studies of the F-dependent decays of $(1s2p)^3P_2$ levels are rare; such studies would still be of interest.
- Theory is relatively complete for Be-like and Mg-like ions but there are few experiments.
- Experimental and theoretical studies of F-dependent rates for Ni-like Xe agree well. Similar studies for other ions would build confidence our understanding.
- Interesting possibilities exist for measuring nuclear quadrupole moments by studying hyperfine quenching in Ti-like ions.

References

1. L. D. Huff and W. V. Houston, Phys. Rev. **36**, 842 (1930).
2. S. Mrozowski, Phys. Rev. **67**, 161 (1945).
3. R. H. Garstang, J. Opt. Soc. Am. **52**, 845 (1962).
4. S. Porsev and A. Derevianko, Phys. Rev. A **69**, 042506 (2004).
5. M. Andersson, Y. Zou, R. Hutton, and T. Brage, J. Phys. B **43**, 095001 (2010).
6. H. Gould, R. Marrus, and P. Mohr, Phys. Rev. Lett. **33**, 676 (1974).
7. L. Engström, C. Jupen, B. Denne, S. Huldt, W. T. Meng, P. Kaijser, J. Ekberg, U. Litzen, and I. Martinson, Physica Scripta **22**, 570 (1980).
8. L. Engström, C. Jupen, B. Denne, S. Huldt, W. T. Meng, P. Kaijser, U. Litzen, and I. Martinson, J. Phys. B **13**, L143 (1980).
9. B. Denne, S. Huldt, J. Pihl, and R. Hallin, Physica Scripta **22**, 45 (1980).
10. E. Jasper, A. Vasilyev, K. Kukla, C. Vogel Vogt, A. E. Livingston, H. G. Berry, S. Cheng, L. J. Curtis, and R. W. Dunford, Physica Scripta **T80**, 466 (1999).
11. A. E. Livingston and S. J. Hinterlong, Nuclear Instruments and Methods **202**, 103 (1982).
12. R. Dunford, C. Liu, J. Last, N. Berrah-Mansour, R. Vondrasak, D. Charles, and L. Curtis, Phys. Rev. A **44**, 764 (1991).
13. R. W. Dunford, H. G. Berry, D. A. Church, M. Hass, C. J. Liu, M. L. A. Raphaelian, B. J. Zabransky, L. J. Curtis, and A. E. Livingston, Phys. Rev. A **48**, 2729 (1993).
14. R. Marrus, A. Simionovici, P. Indelicato, D. Dietrich, P. Charles, J. Briand, K. Finlayson, F. Bosch, D. Liesen, and F. Parente, Phys. Rev. Lett. **63**, 502 (1989).
15. B. Birkett, J. Briand, P. Charles, D. Dietrich, K. Finlayson, P. Indelicato, D. Liesen, R. Marrus, and A. Simionovici, Phys. Rev. A **47**, R2454 (1993).
16. A. Simionovici, B. Birkett, J. Briand, P. Charles, D. Dietrich, K. Finlayson, P. Indelicato, D. Liesen, and R. Marrus, Phys. Rev. A **48**, 1695 (1993).
17. P. Indelicato, B. Birkett, J. Briand, P. Charles, D. Dietrich, R. Marrus, and A. Simionovici, Phys. Rev. Lett. **68**, 1307 (1992).
18. S. Toleikis, E. Berdermann, H. Beyer, F. Bosch, M. Czanta, A. Gumberidze, C. Kozhuharov, D. Liesen, X. Ma, T. Stohlker, et al., Hyperfine Interact. **146**, 139 (2003).
19. S. Toleikis, B. Manil, E. Berdermann, H. Beyer, F. Bosch, M. Czanta, R. Dunford, A. Gumberidze, P. Indelicato, C. Kozhuharov, et al., Phys. Rev. A **69**, 022507 (2004).
20. P. J. Mohr, in *Beam-Foil Spectroscopy*, edited by I. A. Sellin and D. J. Pegg (Plenum, New York, 1976), pp. 97,103.
21. P. Indelicato, F. Parente, and R. Marrus, Phys. Rev. A **40**, 3505 (1989).
22. A. Aboussaïd, M. R. Godefroid, P. Jönsson, and C. Froese Fischer, Phys. Rev. A **51**, 2031 (1995).
23. W. Johnson, K. Cheng, and D. Plante, Phys. Rev. A **55**, 2728 (1997).
24. A. Volotka, V. Shabaev, G. Plunien, G. Soff, and V. Yerokhin, Can. J. Phys. **80**, 1263 (2002).
25. J. Marques, F. Parente, and P. Indelicato, At. Data & Nucl. Data Tables **55**, 157 (1993).
26. F. Parente, J. Marques, and P. Indelicato, Europhys. Lett. **26**, 437 (1994).
27. T. Brage, P. Judge, A. Aboussaïd, M. Godefroid, P. Jönsson, A. Ynnerman, C. Fischer, and D. Leckrone, Ap. J. **500**, 507 (1998).
28. J. Marques, F. Parente, and P. Indelicato, Hyperfine Interact. **146**, 121 (2003), 3rd Euroconference on Atomic Physics at Accelerators, Aarhus, Denmark, SEP 08-13, 2001.
29. J. P. Marques, F. Parente, and P. Indelicato, Eur. Phys. J. D **41**, 457 (2007).
30. M. Andersson, K. Yao, R. Hutton, Y. Zou, C. Y. Chen, and T. Brage, Phys. Rev. A **77**, 042509 (2008).
31. M. Andersson, R. Hutton, and Y. Zou, in *14th International Conference on the Physics of Highly Charged Ions (HCI 2008)*, edited by Azuma, T and Nakamura, N and Yamada, C (2009), vol. 163 of *Journal of Physics Conference Series*, p. 12013.
32. H. Kang, J. Li, C. Dong, P. Jonsson, and G. Gaigalas, J. Phys. B **42**, 195002 (2009).
33. P. Indelicato, Phys. Scr. **T65**, 57 (1996).

34. T. Brage, P. G. Judge, and C. R. Proffitt, *Phys. Rev. Lett.* **89**, 281101 (2002).
35. S. Schippers, E. W. Schmidt, D. Bernhardt, D. Yu, A. Mueller, M. Lestinsky, D. A. Orlov, M. Grieser, R. Repnow, and A. Wolf, in *HCI 2006: 13th International Conference on the Physics of Highly Charged Ions*, edited by McCullough, RW and Currell, FJ and Greenwood, J and Gribakin, G and Scott, MP (2007), vol. 58 of *Journal of Physics Conference Series*, pp. 137–140.
36. S. Schippers, E. W. Schmidt, D. Bernhardt, D. Yu, A. Mueller, M. Lestinsky, D. A. Orlov, M. Grieser, R. Repnow, and A. Wolf, *Phys. Rev. Lett.* **98**, 033001 (2007).
37. T. Rosenband, P. O. Schmidt, D. B. Hume, W. M. Itano, T. M. Fortier, J. E. Stalnaker, K. Kim, S. A. Diddams, J. C. J. Koelemeij, J. C. Bergquist, et al., *Phys. Rev. Lett.* **98**, 220801 (2007).
38. E. Träbert, P. Beiersdorfer, and G. V. Brown, *Phys. Rev. Lett.* **98**, 263001 (2007).
39. C. Schwartz, *Phys. Rev.* **97**, 380 (1955).
40. O. Laporte and W. F. Meggers, *J. Opt. Soc. Am.* **11**, 459 (1925).
41. F. Robicheaux, T. W. Gorczyca, M. S. Pindzola, and N. R. Badnell, *Phys. Rev. A* **52**, 1319 (1995).
42. A. Bohr and V. F. Weisskopf, *Phys. Rev. A* **77**, 97 (1951).
43. I. Savukov and W. Johnson, *Phys. Rev. A* **66** (2002).
44. J. Marques, F. Parente, and P. Indelicato, *Phys. Rev. A* **47**, 929 (1993).
45. K. T. Cheng, A. H. Chen, and W. R. Johnson, *Phys. Rev. A* **77**, 052504 (2008).
46. M. Andersson, Y. Zou, R. Hutton, and T. Brage, *Phys. Rev. A* **79**, 032501 (2009).
47. H. Kang, J. Li, C. Dong, P. Jönsson, and G. Gaigalas, *J. Phys. B* **42**, 195002 (2009).
48. E. Träbert, P. Beiersdorfer, G. V. Brown, K. Boyce, R. L. Kelley, C. A. Kilbourne, F. S. Porter, and A. Szymkowiak, *Phys. Rev. A* **73**, 022508 (2006).
49. E. Träbert, P. Beiersdorfer, and G. V. Brown, *Phys. Rev. Lett.* **98**, 263001 (2007).
50. K. Yao, M. Andersson, T. Brage, R. Hutton, P. Jonsson, and Y. Zou, *Phys. Rev. Lett.* **97**, 183001 (2006).
51. S. Schippers, G. Gwinner, C. Brandau, S. Bohm, M. Grieser, S. Kieslich, H. Knopp, A. Muller, R. Repnow, D. Schwalm, et al., *Nucl. Inst. & Methods in Phys. Res.* **235**, 265 (2005), 12th International Conference on the Physics of Highly Charged Ions, Vilnius, Lithuania, SEP 06-11, 2004.
52. J. P. Marques, F. Parente, and P. Indelicato, *Hyperfine Interact.* **146**, 121 (1955).
53. J. Bieron, P. Indelicato, and P. Jönsson, *Eur. Phys. J - Special Topics* **144**, 75 (2007), 6th Workshop on Atomic and Molecular Physics, Jurata, Poland, Sep, 2006.
54. S. Mannervik, L. Brostrom, J. Lidberg, L. Norlin, and P. Royen, *Phys. Rev. Lett.* **76**, 3675 (1996).